# The effect of gravity on a shaped sonic boom

**T. Cain**
**tcain@gasdynamics.co.uk**
Gas Dynamics Ltd
Farnborough, UK

## ABSTRACT

Previously it was demonstrated that gravity is directly responsible for the attenuation of sonic booms as they propagate towards the ground, while the gradient in acoustic impedance has no effect on the wave strength. This was a significant departure from the well accepted acoustic theory and naturally led to questions concerning comparison with experiment and the implications for low boom design. This paper presents a comparison of measured ground signatures of the Northrup-Grumman Shaped Sonic Boom Demonstrator (SSBD) with a method of characteristics extrapolation from a close proximity flight measurement of static pressure under the aircraft. Comparison is also made with Whitham's theory, extended to include gravity and the ambient temperature variation, as presented in the previous paper. The calculations are both in good agreement with the experimental ground signature. The usual equations that define the acoustic propagation (gravitational body force neglected) are transformed so that the computational algorithms of the extended Whitham theory are applicable. The transformation simplifies the acoustic model and reveals the conditions under which the errors in its prediction will be large. At the Mach number of 1.4, corresponding to the SSBD flight, the error is relatively small and the acoustic prediction is also in close agreement with the ground signature.

## NOMENCLATURE

| | |
|---|---|
| $a$ | speed of sound ($ms^{-1}$) |
| $C_p$ | specific heat of cool air at constant pressure (1004 $J.kg^{-1}K^{-1}$) |
| $F$ | Whitham's function ($m^{1/2}$) |
| $g$ | local gravity ($ms^{-2}$) |
| $G$ | advance factor, Equation 13 ($m^{1/2}$) |
| $h$ | geopotential altitude (m) |
| $H$ | potential function, Equation 4 ($J.kg^{-1}$) |
| $k$ | function of M, Equation 11 |
| $L$ | reference length (m) |
| M | free stream Mach number |
| $p$ | pressure (Pa) |
| $q$ | radial function, Equation 8 ($m^{-1/2}$) |
| $qA$ | acoustic radial function, Equation 20 ($m^{-1/2}$) |
| $r$ | radius (m) |
| $R$ | gas constant of air (287 J.kg-1.$K^{-1}$) |
| $S$ | entropy ($J.kg–1.K^{-1}$) |
| $t$ | time, or running variable (s, or m) |
| $T$ | temperature (K) |
| $u$ | $x$ component of velocity ($ms^{-1}$) |
| $u^\wedge$ | perturbation of $u$ ($ms^{-1}$) |
| $V$ | total velocity ($ms^{-1}$) |
| $x$ | horizontal axis, positive from nose to tail (m) |
| $\chi$ | $x$-co-ordinate of characteristics intercept (m) |
| $\beta$ | $\sqrt{M^2-1}$ |
| $\gamma$ | ratio of specific heats for cool air (7/5) |
| $\theta$ | Streamline angle about $y$ (rad) |
| $\mu$ | Mach angle (rad) |
| $\rho$ | density ($kg.m^{-3}$) |

### Subscripts

| | |
|---|---|
| 1, 2, .. | state at some fixed radius, $r_1$, $r_2$, ... |
| $A$ | acoustic theory |
| $c$ | on the characteristic |
| $f$ | at flight altitude |
| ref | reference |
| $\infty$ | unperturbed value, can be a function of altitude |

**Paper No. 3474**. Manuscript received 1 July 2009, revised 30 March 2010, accepted 15 April 2010.

https://doi.org/10.1017/S0001924000004127 Published online by Cambridge University Press



Figure 1. F-15B measured static pressure in close proximity to the SSBD in supersonic flight, Flight 8, 25 August 2003, Photograph EC03-0225-5 courtesy of NASA.

## 1.0 INTRODUCTION

Proof that gravity is directly responsible for the attenuation of sonic booms and that the density gradient within a hydrostatic atmosphere has no direct effect, was presented in a recent paper[1]. That paper challenged the assumptions on which most boom prediction codes are based; these typically omit gravity from the acoustic propagation equations but include an artificial acoustic impedance effect. Although these codes have achieved a satisfactory match with ground pressure measurements in the past, this does not guarantee that the acoustic theory is applicable to the design of low boom aircraft, or that it can be applied at conditions different than those for which agreement with experiment has been found satisfactory. In this paper, signature predictions from the new extended Whitham theory (EWT) are tested by comparison with those from the method of characteristics (MOC) and the measured signature of the Northrup-Grumman Shaped Sonic Boom Demonstrator (SSBD)[2]. Comparison is also made with predictions based on geometric acoustics by transformation of the acoustic equations into a form compatible with EWT. The transformation reveals the conditions under which the error in the flawed acoustic theory becomes large.

## 2.0 NEAR FIELD SIGNATURES

The Shaped Sonic boom Demonstrator flights in August 2003 were followed by a series of flights in January 2004 within a new programme named the Shape Sonic Boom Experiment (SSBE). An overview of the programmes is given by Palowski *et al*[2], in a freely available reference that helps put into context the near field data presented by Haering and Murray[3] and the ground signatures presented by Plotkin *et al*[4]. The present author had no connection with the SBBD/E programmes and all the data presented here is drawn from these three references.

Flight 30 on 20 January 2004 involved an F-15B fitted with a nose probe measuring static pressure while flying directly below the SSBD. Figure 1 shows the aircraft in close proximity flight during the August campaign. Mach number was limited by the summer temperatures in combination with the extra drag of the SSBD forebody in comparison to the underlying sleek airframe of the F-5E. The design Mach number of 1·4 was achieved in winter and Fig. 2 shows static pressure pressures measured directly below the aircraft at a nominal vertical separation of 30·5m. Also on the figure is a record[3] of pressure disturbance below an unmodified F-5E obtained on 4 March 2002. Although not given, the distance below the aircraft is calculated to be 26m from the relative position of the bow shock (24m), and by noting that the bow shock has advanced 2m ahead of the Mach line for the SSBD at the same separation.

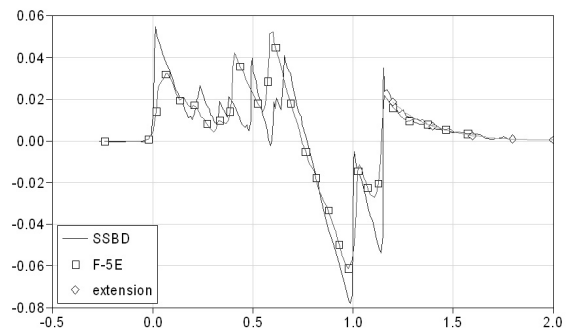



Figure 2. Normalised static pressure perturbation 30m below the SSBD and 26m below the F-5E. The extension corresponds to Equation 1.

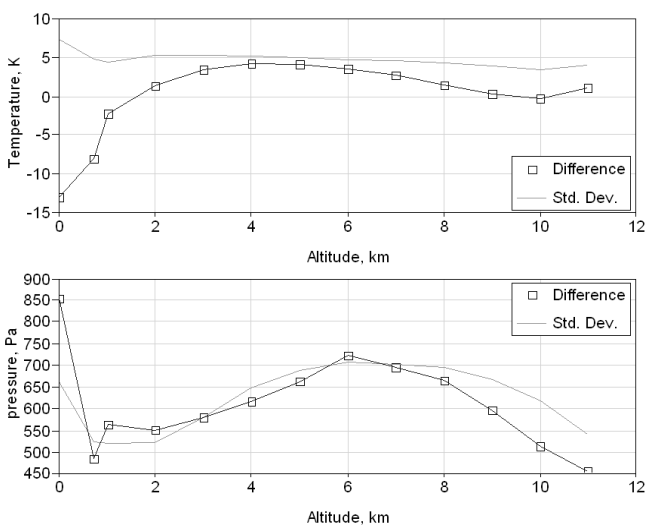



Figure 3. Mean departures from the US Standard atmosphere (1976) at Edwards AFB6 during January and the magnitude of the standard deviation for that month.

These signatures provide the initial conditions for all three prediction methods. The reference length, $L$ = 14·68m, is the length of the F-5E5, although of course the reference length affects only the presentation of the data and any length could have been used.

In order to trace the tail shock to the ground, the near field signatures needed a short extension as the characteristic from the last data point catches the tail shock before the ground. The curve defined by,

$$F = 0{\cdot}0007\exp(5(1{\cdot}5 - \chi/L)) \quad \ldots \quad (1)$$

and shown in green is used for both wakes, where $\chi$ is greater than the measured signature limit.

## 3.0 ATMOSPHERE

The measured static pressure perturbations have been normalised by the ambient pressure at the altitude of the measurement, and this is has been assumed equal to the value from the US Standard atmosphere (1976). The atmosphere over Edwards, in January, is on average reasonably close to this standard. The differences from the 1976 standard, of the calculated mean for January[6] is plotted in Fig. 3 along with the magnitude of the standard deviation from this mean. Since the departures in temperature and pressure are not more than about one standard

https://doi.org/10.1017/S0001924000004127 Published online by Cambridge University Press

deviation, the standard atmosphere was used in all the calculations reported here. Although wind may have affected the ground signature and could have been accounted for, at least in the MOC prediction, it only make sense to do so if the flight heading and meteorological measurements were publicly available, hence a still atmosphere is assumed. The assumption of a quiescent standard atmosphere might also enable the results presented here to be reproduced more easily.

## 4.0 MOC EXTRAPOLATION

As described in the previous paper the compatibility relations for characteristics in the axisymmetrical flow at sufficient distance from the aircraft are[7]:

$$\mathrm{Cot}\mu\frac{\mathrm{d}V}{V}\mp\mathrm{d}\theta+\frac{\mathrm{Cot}\mu}{V^2}\left(T\mathrm{d}S-\mathrm{d}H\right)-\frac{\mathrm{Sin}\theta\,\mathrm{Sin}\mu\,\mathrm{d}r}{\mathrm{Sin}\left(\theta\pm\mu\right)}\left(\frac{1}{r}+\frac{g}{a^2}\right)=0 \quad \ldots (2)$$

where the characteristics are the Mach lines

$$\frac{\mathrm{d}r}{\mathrm{d}x}=\mathrm{Tan}\left(\theta\pm\mu\right) \quad \ldots (3)$$

The inclusion of gravity in Equation 2 implies a cylindrical gravitational field radiating outward from the centreline. Fortunately the gravitational term is small compared to the $1/r$ term until a radius of about $a^2/g/10$ = 0·9km, and at such a radius the circumferential gradients due to the relative inclination of the gravity vector are almost certainly negligible in comparison to other gradients over the 30m axial length of the disturbance.

Gravity also appears within the potential term $H$, which combines the streamlines total enthalpy with its undisturbed gravitational potential.

$$H\left(x,r\right)=H\left(h_\infty\right)=C_p\left(T_\infty-T_{ref}\right)+\frac{1}{2}\left(u_\infty^2-u_{ref}^2\right)+g_{ref}\left(h_\infty-h_{ref}\right). \ldots (4)$$

Here for convenience the geopotential height, $h_\infty$, is used rather than the altitude as by its definition it allows the above simple expression for gravitational potential energy while still allowing for variation of gravitational acceleration with altitude. The entropy of the air on each streamline is simply determined by its initial value at height $h_\infty$ with the addition of the entropy increase across each upstream shock.

$$S\left(x,r\right)=S\left(h_\infty\right)+\sum\Delta S=C_p\log\left(\frac{T_\infty}{T_{ref}}\right)-R\log\left(\frac{p_\infty}{p_{ref}}\right)+\sum\Delta S \quad \ldots (5)$$

Thus the differential sum within the third term of the compatibility relation reduces to,

$$TdS-dH=T\sum\Delta S-u_\infty du_\infty \quad \ldots (6)$$

The first term is due to shocks upstream of the point on the streamline and the second would normally be zero although it could be used to explore the effect of wind in the direction of flight.

Note how the compatibility relation for two dimensional steady flow is unaffected by the pressure gradients within a hydrostatic atmosphere. Although this lack of sensitivity to pressure may seem fortuitous, it is in fact inevitable. Consider the compatibility relation when the 'aircraft' produces no disturbance and hence streamline angles are zero everywhere. In the case of no wind, d$V$ is zero and the third term must also be zero. In the case of wind, the first and third terms are equal and opposite.

The complete insensitivity of the wave propagation to the atmospheric gradients, prompted the re-evaluation of the acoustic theory for which density gradients play such a large role, as presented in the previous paper1.

Numerical solutions of the compatibility equations are presented in Fig. 4 for the SSBD and F-5E. The rapid formation of the $N$ Wave in the case of the F-5E is apparent, whereas the SSBD preserves

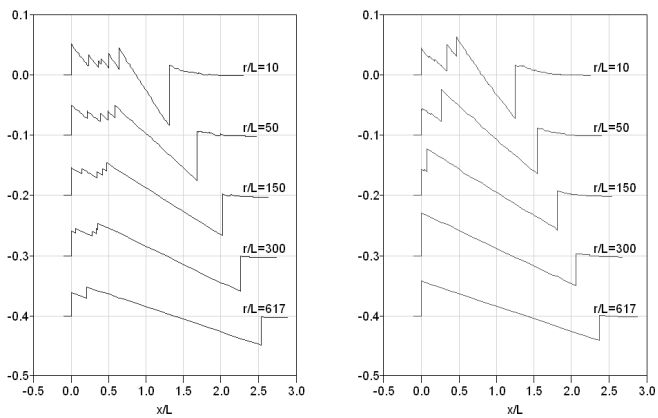



Figure 4. MOC calculated signature development of the SSBD (left) and F-5E (right) for Mach 1·4 flight at 9754m (32kft). The ground at 702m above mean sea level, is at $r/L$ = 617.

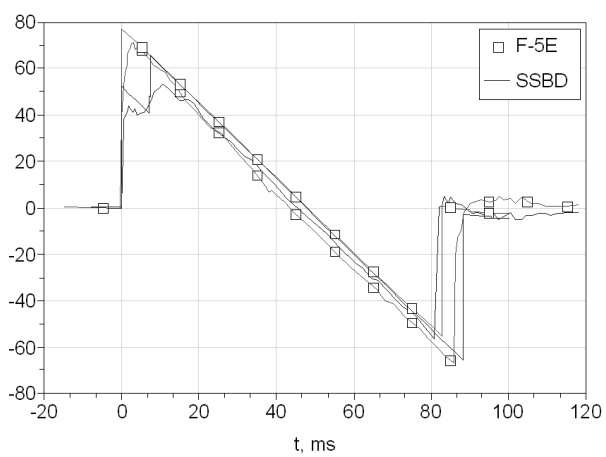



Figure 5. Measured (Flight 15, Fig. 6)[4] and MOC signatures (dashed) for the SSBD and F-5E, assuming a ground reflection factor of 1·8.

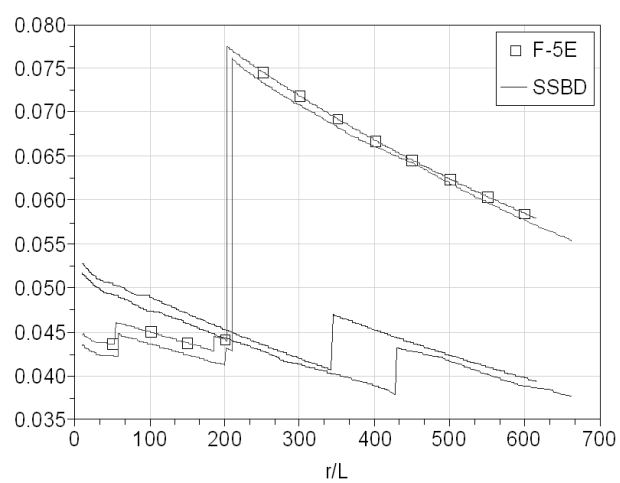



Figure 6. Bow shock overpressure for the SSBD and F-5E as calculated with MOC (dashed) and EWT (solid ).

https://doi.org/10.1017/S0001924000004127 Published online by Cambridge University Press

some character to the ground. Comparison with the signatures measured on the ground is satisfactory, Fig. 5, with a reflection factor of 1·8 (90% of the specular value).

## 5.0 EXTENDED WHITHAM THEORY

In the previous paper it was demonstrated that when the perturbations are small the compatibility relation (Equation 2) can be integrated along a characteristic to give,

$$\frac{\hat{u}}{u_\infty} = -F(\chi)\frac{q(r)}{\sqrt{2\beta}} \qquad \ldots (7)$$

where,

$$q(r) = \left(\frac{p_1}{p}\right)^{\frac{1}{2\gamma}} \frac{1}{\sqrt{r}} \qquad \ldots (8)$$

is a function representing the radial dependence that includes the effect of gravity.

$F(\chi)$ is Whitham's function and its value on each characteristic may be calculated from the aircraft geometry, as demonstrated by Whitham[8] and Walkden[9], or it may be calculated directly from Equation 7 if the perturbation in pressure has been measured since,

$$\frac{\Delta p}{p} = -\gamma \mathrm{M}(r)^2 \frac{\hat{u}}{u_\infty} = \gamma \mathrm{M}(r)^2 F(\chi)\frac{q(r)}{\sqrt{2\beta}} \qquad \ldots (9)$$

The local slope of the characteristic is,

$$\frac{\partial x_c}{\partial r} = \beta(r) - \frac{1}{2}F(\chi)k(r)q(r) \qquad \ldots (10)$$

where,

$$k = (\gamma+1)\mathrm{M}^4/\sqrt{2\beta^3} \qquad \ldots (11)$$

The Mach number dependence of $k$ makes it also radius dependent. Integrating along the characteristic between $r_1$ and $r_2$,

$$x_{c2} - \chi = \int_{r_1}^{r_2} \beta \,\mathrm{d}r - \frac{F(\chi)}{2}\int_{r_1}^{r_2} k\,q\,\mathrm{d}r = \int_{r_1}^{r_2} \beta\,\mathrm{d}r - \frac{1}{2}F(\chi)G(r) \qquad \ldots (12)$$

where the $x$ co-ordinate of the characteristic at $r_1$ has defined $\chi$. This is a departure from Whitham's definition[8] in which $\chi$ is the characteristics $x$-co-ordinate on the axis. To recover Whitham's result $r_1$ can be taken as zero. When extrapolating from CFD, wind tunnel data or flight data, it is more convenient, and more accurate, to start the characteristics at a radius sufficiently large that both: three dimensional effects are negligible; and the velocity perturbations are well described by small perturbation theory.

Note that the advance factor $G$ is defined here as,

$$G(r_2) = \int_{r_1}^{r_2} k\,q\,\mathrm{d}r \qquad \ldots (13)$$

and as seen from Equation 12, $G$ is equal to twice the advance of a characteristic of unit strength $F$. Advance is a term common to both Whitham and acoustic theories, and refers to the relative position of a characteristic in comparison to a hypothetical one that originates at the same position but whose slope is always set by the local free stream Mach angle.

As demonstrated in the previous paper, Whitham's method for locating the characteristic that intersects the bow shock at radius $r$, still applies for non uniform atmospheres, and hence $F$ at the bow shock is determined by,

$$F(\chi)^2 = \frac{4}{\mathrm{G}(r)}\int_0^x F\,\mathrm{d}t \qquad \ldots (14)$$

Although Whitham remarked that this simple formula would require modification if downstream shocks caught up to the bow shock[8], actually it does apply unconditionally. This can be demonstrated by considering the two constraints that define shock formation within an $F$-curve. The first is that the characteristics upstream and downstream of the shock are co-located and therefore from Equation 12,

$$\chi_a - \chi_b = G(r)\left(F(\chi_a) - F(\chi_b)\right)/2 \qquad \ldots (15)$$

and the second constraint, is that the area under the $F$-curve absorbed within the shock is equal to the area under the straight line that links the shocks upstream and downstream characteristics on the $F$-curve. That is[8],

$$\int_{\chi_a}^{\chi_b} F\,\mathrm{d}t = (\chi_a - \chi_b)\left(F(\chi_a) - F(\chi_b)\right)/2 \qquad \ldots (16)$$

This last constraint follows from the fact that a weak shock advances at the mean of the rate of the characteristics immediately upstream and downstream. Substitution of Equation 15 into 16 reveals,

$$F(\chi_b)^2 - F(\chi_a)^2 = \frac{4}{G(r)}\int_{\chi_a}^{\chi_b} F\,\mathrm{d}t \qquad \ldots (17)$$

Thus, as previously noted by Whitham, the bow shock is just the specific case of a general shock, in which $F(\chi_a) = 0$ and the area under the $F$-curve upstream of $\chi_a$ is also zero. That is, $\chi_a$ is upstream of the aircraft on a characteristic in the free stream.

One should also note from Equation 17, that when a shock linking the characteristics $\chi_a$ and $\chi_b$ arrives at the bow shock, the resulting jump in $F^2$ exactly compensates for the area lost under the $F$-curve. Thus the bow shock strength can always be calculated directly from Equation 14, without concern for any shocks that may have caught the bow shock.

Pressure jump across the bow shock calculated from Equation 14 is compared with the MOC calculation in Fig. 6 for the SSBD and F-5E. Agreement is very good although there is a discrepancy between the methods in the case of the SSBD signature near the radius of 400$L$. MOC predicts a delayed arrival of one of the downstream shocks, stemming from minor differences in the interpolation of the initial $F$-curve. A comparison of the entire signature at 400$L$ is made in Fig. 7. Although the difference in bow shock pressure jump is greater than 10%, the variation is associated with a very small difference, 0·0116L (17cm) in the second shock position. Close agreement in pressure levels in parts of the signature away from shocks, with some small differences in predicted shock positions is evident in the downstream parts of the signatures, Fig. 7. Shocks in the EWT calculation are identified by simultaneous solution of Equations 15 and 16. They necessarily are located on the negative slopes of the $F$-curve and on a highly irregular curve like that associated with the SSBD in Fig. 2, there is inevitably some sensitivity to the interpolation method. However in practice, these differences are minor in comparison to the distortions introduced by passage of the wave system through the atmospheres boundary layer. Note that there is no accumulation of error as each shock is located independently of the others, and in EWT the signature at each radial location is calculated independently, requiring only the initial $F$-curve and the integral $G$.

MOC and EWT signatures are compared at other radii in Fig. 8. Shocks are marked on the initial $F$-curve for the SSBD by linking the upstream and downstream characteristics with a straight line; the slope of this line being just 2/$G$ (Equation 15).

https://doi.org/10.1017/S0001924000004127 Published online by Cambridge University Press

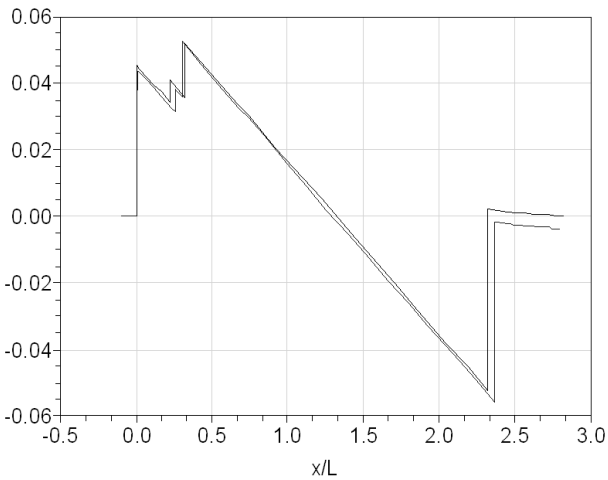



Figure 7. SSBD Pressure signature at *r*/*L*=400 as calculated with MOC (dashed) and EWT.

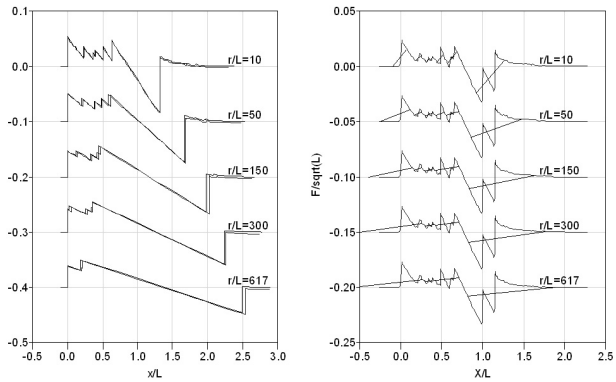



Figure 8. MOC and EWT (dashed) signature prediction for the SSBD. Right hand figure shows shock locations on the SSBD initial *F*-curve.

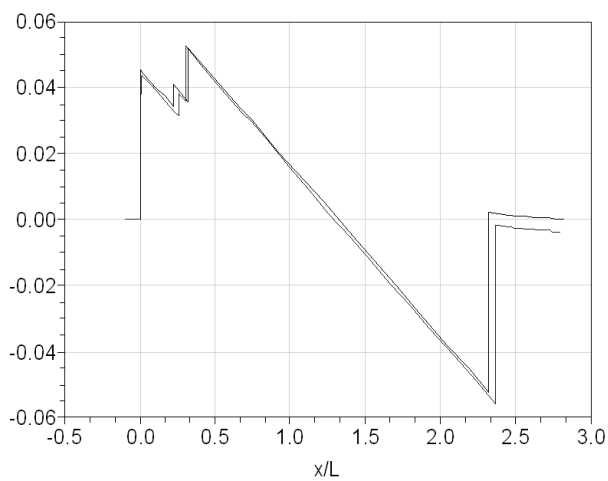



Figure 9. Measured (Flight 15, Fig. 6)[4] and acoustic theory signatures (dashed) for the SSBD and F-5E, assuming a ground reflection factor of 1·8.

## 6.0 ACOUSTIC THEORY

As previously explained1 the acoustic theory of sonic boom is based on a false premise. That is, that increasing acoustic impedance is responsible for the attenuation of the wave as it propagates towards the ground. This results in the relationship[10],

$$\Delta p = \sqrt{\frac{\rho a A_1}{\rho_1 a_1 A}}\Delta p_1 \qquad \ldots (18)$$

describing transmission of a plane acoustic wave down an imaginary tube of area $A$. The area of this tube is determined by considering the diffraction of its boundaries due to the gradient in the speed of sound. Application of Snell's law results in[10],

$$\frac{A}{A_1} = \frac{a\beta}{r_1 a_1}\int_0^r \frac{\mathrm{d}r}{\beta} \qquad \ldots (19)$$

In every other respect the acoustic treatment of the wave system is identical to Whitham theory. Replacing $q$ with $q_A$ defined as

$$q_A = \sqrt{\frac{\rho_1}{\rho}}\left(\beta_1 \int_0^r \frac{\mathrm{d}r}{\beta}\right)^{\frac{1}{2}} \qquad \ldots (20)$$

allows direct application of the equations and algorithms developed for EWT, and a demonstration of the error that results from the assumptions behind Equations 18 and 19. For example, in an isothermal atmosphere the acoustic theory predicts an attenuation that is significantly greater than EWT, differing by the exponent ?. Hence if EWT were to indicate a factor of two attenuation (along a characteristic) due to gravity then the acoustic theory would indicate a factor $2^{1.4} = 2{\cdot}64$.

The SSBD programme was intended as a test of the acoustic theory's application to shaped sonic booms. The flawed theory does a remarkably good job at predicting the ground signature of both the SSBD and F-5E, Fig. 9. Such agreement between theory and experiment leaves the theory unchallenged and may in part explain why its inherent problem went undetected for half a century.

## 7.0 IMPLICATIONS FOR LOW BOOM DESIGN

Evolution of signature shape is solely determined by the advance factor $G$. Pressure level along any particular characteristic is determined by local free stream conditions and $q$. Therefore these two parameters essentially determine whether efforts to minimise sonic boom will be successful, at least with respect to propagation.

Apart from the MOC analysis of Ferri[11] and Darden[7], all other known sonic boom studies have relied on acoustic theory to predict signature development. Comparison of $q$ and $G$ from acoustic theory with that from EWT allows a direct assessment of the errors that have resulted from its application. The errors are a function of flight Mach number and altitude, but since optimum wing loading tends to dictate supersonic cruise flight at an equivalent airspeed near 400kt (a dynamic pressure of 26kPa), representative errors are presented as a function of Mach number for flight at this dynamic pressure in Fig. 10.

Acoustic $G$ varies from 95 to 90% of the actual value of $G$ at ground level as flight Mach number increases from 1·4 to 3·5. Therefore the strength of the characteristic, $F$, at the bow wave which varies with the square root of $G$ (Equation 14) is well estimated by the acoustic theory. However the pressure jump which is proportional to the product $Fq$ is significantly underestimated at the higher Mach numbers, being only 65% of the actual level at Mach 4.

Advance factor $G$, (the $kq$ integral), plays a significant role in signature shape; As noted before, $2/G$ is the slope of the line on an $F$-curve that connects the characteristics immediately upstream and downstream of a shock. For precisely the same reason the divergence of characteristics from a point on the negative slope of an $F$-curve is just $-2/G$ and the rate of pressure decrease in an $N$-wave at any altitude is just,

https://doi.org/10.1017/S0001924000004127 Published online by Cambridge University Press

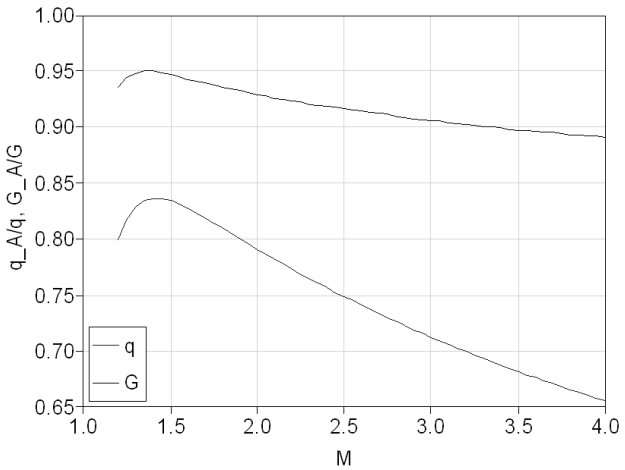



Figure 10. Error in the acoustic theory for flight at 400KEAS.

$$\frac{dp}{dt} = \frac{-2u_f^3 \rho q}{G\sqrt{2\beta}} \quad \ldots (21)$$

as readily seen by differentiation of Equation 11, substituting pressure for $F$ from Equation 8 and noting that characteristics that make up this portion of the wave originate very close to each other (a common $\chi$). These are Whitham's arguments[8], simply updated to include the non-uniform atmosphere with all the parameters in Equation 21 calculated at the wave altitude.

The slope of the pressure signal for a sonic boom recorded on the ground is only slightly underestimated at low Mach numbers with the acoustic theory, since both $q$ and $G$ are low. In fact one could not discern from Figs 5 and 9 whether EWT or the acoustic theory is in better agreement with the experiment; A reflection factor of 2 rather than 1·8 would account for the difference in slope that is observed in Fig. 9. Once again, it is this consistency with experiment that no doubt contributed to acceptance of the acoustic theory. However boom minimisation by signature shaping requires an accurate theory. This can be appreciated by close examination of Fig. 8. The significantly reduced bow shock pressure of the SSBD in comparison to the F-5E is due to a delay in the arrival of a downstream shock, but this was the result of a relatively fine balance of the $F$-curve in which the bow shock strength is being controlled by just the front quarter of the aircraft. That is, the characteristic at the bow wave originates at $\chi/L$ = 0·275 (4m or 13ft) as can be seen from the right hand side of figure 8 for $r/L$ = 617. This axial station is just downstream of the start of the SSBD cockpit canopy. Even if the aircraft had terminated there the resulting relatively slender, short body would have produced the same bow shock pressure as the SSBD and this was a factor of 2 to 3 above what might be considered acceptable; illustrating the extent of the challenge quiet supersonic flight poses.

## 8.0 CONCLUSIONS

Sonic boom signatures calculated with MOC, EWT and acoustic theory are all in close agreement with the measured SSBD and F-5E signatures. Satisfactory match with ground pressure measurements is one of the reasons acoustic theory has gone unchallenged despite the fact that gravity and not increasing acoustic impedance is responsible for the attenuation of pressure waves as the they travel from the aircraft to the ground. Transformation of the acoustic model into a form equivalent to the recently extended Whitham theory allowed the determination of flight conditions under which the error in the acoustic model predictions will be most significant. Acoustic theory was shown to underestimate both overpressure and the rate at which characteristics in a compressive region converge.

## ACKNOWLEDGEMENT

This work was performed within the Aerodynamic and Thermal Load Interactions with Lightweight Advanced Materials for High Speed Flight project investigating high-speed transport. ATLLAS, coordinated by ESA-ESTEC, is supported by the EU within the 6th Framework Programme Priority 1.4, Aeronautic and Space, Contract no.: AST5-CT-2006-030729. Further info on ATLLAS can be found on http://www.esa.int/techresources/atllas.

## REFERENCES

1. CAIN, T. A correction to sonic boom theory, *Aeronaut J*, **113**, (1149), pp 739-745;
2. PAWLOWSKI, J., GRAHAM, D., BOCCCADORO C., COEN, P. and MAGLIERI, D. Origins and overview of the shaped sonic boom demonstration program, January 2005, AFRL-VA-WP-TP-2005-300 (includes AIAA-2005-5), ADA440153, DTIC.
3. HAERING E. and MURRAY J. Shaped sonic boom demonstration/experiment airborne data, 2004, Shaped sonic boom demonstration final review, NASA Langley Research Center, 17 August 2004, Document 20070023459, NTRS.
4. PLOTKIN, K., HAERING, E., MURRAY, J., MAGLIERI, D., SALAMONE, J., SULLIVAN, B. and SCHEIN, D. Ground data collection of shaped sonic boom demonstration aircraft pressure signatures, 2005, AIAA-2005-0010, 43rd AIAA Aerospace Sciences Meeting and Exhibition, 10-13 January 2005, Reno, NV, USA|.
5. SCHER, S. and WHITE, W. Spin-tunnel investigation of a 1/20-scale model of the Northrop F-5E airplane, 1977, NASA-TM-SX-3556.
6. Meteorology Group, Range reference atmosphere 0-70km altitude, Edwards AFB, California, 1983, Document 366-83, ADA132487, DTIC.
7. DARDEN, C. An analysis of shock coalescence including the tree-dimensional effects with application to sonic boom extrapolation, 1984, NASA-TP-2214.
8. WHITHAM, G.B. The flow pattern of a supersonic projectile, *Communications on Pure and Applied Mathematics*, 1952, **5**, pp 301-348.
9. WALKDEN, F. The shock pattern of a wing-body combination far from the flight path, *Aeronaut Q*, May 1958, **9**, part 2, pp 164-194.
10. GEORGE, A. and PLOTKIN, K. Sonic boom waveforms and amplitudes in a real atmosphere, *AIAA J*, 1969, **7**, (10), pp 1978-1981.
11. FERRI, A., TING, L. and LO, R. Nonlinear sonic-boom propagation including the asymmetric effects, *AIAA J*, **15**, (5), 1977, pp 653-658.

https://doi.org/10.1017/S0001924000004127 Published online by Cambridge University Press